Intestinal epithelial apoptosis initiates gut mucosal injury during extracorporeal membrane oxygenation in the newborn piglet

Krishnan MohanKumar[1,2], Cheryl R Killingsworth[3], R Britt McIlwain[4], Joseph G Timpa[4], Ramasamy Jagadeeswaran[1,2], Kopperuncholan Namachivayam[1,2], Ashish R Kurundkar[5], David R Kelly[5], Steven A Garzon[6] and Akhil Maheshwari[1,2,7]

Neonates and young infants exposed to extracorporeal circulation during extracorporeal membrane oxygenation (ECMO) and cardiopulmonary bypass are at risk of developing a systemic inflammatory response syndrome with multi-organ dysfunction. We used a piglet model of ECMO to investigate the hypothesis that epithelial apoptosis is an early event that precedes villous damage during ECMO-related bowel injury. Healthy 3-week-old piglets were subjected to ECMO for up to 8 h. Epithelial apoptosis was measured in histopathological analysis, nuclear imaging, and terminal deoxynucleotidyl transferase dUTP nick end labeling. Plasma intestinal fatty acid-binding protein (I-FABP) levels were measured by enzyme immunoassay. Intestinal mast cells were isolated by fluorescence-assisted cell sorting. Cleaved caspase-8, caspase-9, phospho-p38 MAPK, and fas ligand expression were investigated by immunohistochemistry, western blots, and reverse transcriptase-quantitative PCR. Piglet ECMO was associated with increased gut epithelial apoptosis. Extensive apoptotic changes were noted on villus tips and in scattered crypt cells after 2 h of ECMO. After 8 h, the villi were denuded and apoptotic changes were evident in a majority of crypt cells. Increased circulating I-FABP levels, a marker of gut epithelial injury, showed that epithelial injury occurred during ECMO. We detected increased cleaved caspase-8, but not cleaved caspase-9, in epithelial cells indicating that the extrinsic apoptotic pathway was active. ECMO was associated with increased *fas* ligand expression in intestinal mast cells, which was induced through activation of the p38 mitogen-activated protein kinase. We conclude that epithelial apoptosis is an early event that initiates gut mucosal injury in a piglet model of ECMO.

Neonates and young infants exposed to extracorporeal circulation during extracorporeal membrane oxygenation (ECMO) and cardiopulmonary bypass (CPB) are at high risk of developing a systemic inflammatory response syndrome (SIRS) with multi-organ dysfunction.[1–4] CPB is used frequently during cardiothoracic surgery to obtain a non-beating, bloodless heart, whereas ECMO is a life-support system of last resort used to provide oxygenation and/or circulatory support in infants with intractable cardiorespiratory failure because of diverse causes, such as persistent pulmonary hypertension of the newborn, meconium aspiration syndrome, sepsis, and heart defects.[5] Understanding ECMO/CPB-related SIRS is critical for the development of anti-inflammatory strategies that may reduce associated morbidity.

To investigate the mechanisms of extracorporeal circulation-related SIRS, we have developed a porcine neonatal model of ECMO where we subject previously healthy 3–6 kg weighing piglets to venoarterial ECMO.[6,7] Piglet ECMO is associated with inflammatory changes similar to those reported in human studies, including hemodynamic changes, leukocyte activation, increased expression of inflammatory

[1]Division of Neonatology, Department of Pediatrics, University of Illinois at Chicago, Chicago, IL, USA; [2]Department of Pediatrics, Center for Neonatal and Pediatric Gastrointestinal Disease, University of Illinois at Chicago, Chicago, IL, USA; [3]Animal Resources Program, University of Alabama at Birmingham (UAB), Birmingham, AL, USA; [4]University Hospital Services, University of Alabama at Birmingham (UAB), Birmingham, AL, USA; [5]Department of Pathology, University of Alabama at Birmingham (UAB), Birmingham, AL, USA; [6]Department of Pathology, University of Illinois at Chicago, Chicago, IL, USA and [7]Department of Pharmacology, University of Illinois at Chicago, Chicago, IL, USA
Correspondence: Dr A Maheshwari, MD, Department of Pediatrics, University of Illinois at Chicago, 840S Wood Street, CSB 1257, UIC m/c 856, Chicago, IL 60612, USA.
E-mail: akhil1@uic.edu
Received 9 September 2013; revised 8 November 2013; accepted 9 November 2013

cytokines, and microvascular injury in diverse organs such as lung, intestine, liver, and kidney.[6] In this model, disruption of the intestinal epithelial barrier, histopathological evidence of epithelial damage, and bacterial translocation are prominent findings. However, it remains unknown whether the observed loss of intestinal epithelium underlies the gross tissue necrosis, or only coincides with the widespread gut mucosal injury during ECMO. In this study, we investigated the hypothesis that epithelial apoptosis is an early event that precedes villous damage during ECMO-related gut mucosal injury.

METHODS
Neonatal Piglet ECMO
Mixed-breed neonatal piglets of either gender weighing 3–6 kg were subjected to venoarterial ECMO as previously described.[6,7] Animal studies were performed at University of Alabama at Birmingham after obtaining approval from the Institutional Animal Care and Use Committee. During ECMO, the piglets received general anesthesia and mechanical ventilation (volume-controlled, tidal volume 10–15 ml/kg, 10–15 cycles/min, $FiO_2 = 21\%$; Hallowell EMC 2000 ventilator) to maintain acceptable arterial blood gases ($pO_2 = 70$–150 mm Hg, $pCO_2 = 35$–45 mm Hg, and pH = 7.35–7.45). Biomedicus 8F cannulae (Medtronic, Minneapolis, MN, USA) were inserted into the external jugular vein and the external carotid artery. Animals were heparinized to maintain activated clotting times of 180–220 s. The ECMO system consisted of a Biomedicus BP-50 centrifugal pump (Medtronic, Shoreview, MN, USA) and a Minimax hollow fiber oxygenator (Medtronic). Gas flow rates were maintained in the oxygenator at 0.5 l/min 100% oxygen. After starting ECMO, flow rates in the circuit were advanced to 250 ml/min or 1.5 l/min/m^2. Sham animals received anesthesia, ventilation, cannulation, and heparinization similar to ECMO animals, but were not connected to the circulatory pump device. Data in this study represent five animals each in sham and ECMO groups that were killed after 2 h, and eight animals each in sham and ECMO groups killed after 8 h.

Nuclear Morphology
Tissue sections were deparaffinized using the EZ-AR common solution (Biogenex, San Remon, CA, USA) per manufacturer's protocol and nuclear staining was obtained with 4′,6-diamidino-2-phenylindole (DAPI; 1:1000 × 3 min; Calbiochem, San Diego, CA, USA). Nuclei with apoptotic changes such as chromatin condensation and/or fragmentation[8] were enumerated using a Zeiss Axiovert fluorescence microscope. Chromatin condensation was defined as coalescence of chromatin into distinct clumps localized mostly at the nuclear periphery and resulting in central 'cavitation'. We also performed nuclear morphological analysis using a previously described software plugin[9] for Image J, a public-domain image-processing program developed at the National

Institutes of Health.[10] We measured nuclear area, aspect (ratio between the major and minor radii of the nucleus), area/box (ratio between nuclear area and the area of its bounding box), radius ratio (ratio between the maximum and the minimum nuclear radii), and roundness (computed as perimeter^2/($4 \times \pi \times$ area), where π is the mathematical constant.[9] Nuclear irregularity index (NII) was defined as [aspect—(area/box) + radius ratio + roundness].[9] In this analysis, decreased nuclear area and lower values of the NII are associated with apoptosis.

Terminal Deoxynucleotidyl Transferase-Mediated dUTP Nick End Labeling (TUNEL)
TUNEL staining was performed to detect apoptotic changes in the intestine of sham and ECMO animals. We used a commercially available kit (Roche, Indianapolis, IN, USA) per manufacturer's instructions. Briefly, deparaffinized sections were treated with proteinase K (15 µg/ml) for 15 min and then rinsed with PBS. Endogenous peroxidase was inactivated by immersing in 3% H_2O_2 for 5 min. Sections were then immersed in a buffer containing deoxynucleotidyl transferase and fluorescein-deoxy-Uridine triphosphate for 90 min at 37 °C in 100% relative humidity. After washing with PBS, the sections were incubated with an Alexa fluor 488-conjugated anti-fluorescein antibody for 30 min. Imaging was performed using the Zeiss Laser scanning microscope 510-Meta microscope.

Severity of Epithelial Cell Apoptosis and Villous Disruption
Serial tissue sections stained with H&E and for TUNEL were scored by a blinded observer for the severity of epithelial cell apoptosis and villous damage, respectively. In TUNEL-stained sections, score 0 = intact villous epithelium, sporadic TUNEL$^+$ nuclei; 1 = clusters of TUNEL$^+$ nuclei on villus tips; 2 = TUNEL$^+$ nuclei covering the villus but not seen in crypts; 3 = TUNEL$^+$ nuclei penetrating into the crypts; and 4 = TUNEL$^+$ nuclei all along the crypt-villus axis.[11] Villous damage was scored similarly: score 0 = intact villi; 1 = sloughing of cells on villus tips; 2 = mid-villus damage; 3 = loss of villi but crypts can be recognized; and 4 = both villi and crypts cannot be recognized. Ten fields were examined per section ($n = 5$ animals/group) and highest scores were recorded in each microscopic field.

Immunohistochemistry
We used our previously described protocol for immunohistochemistry.[6,7] Briefly, tissue sections were deparaffinized, treated with Proteinase K (20 µg/ml; Promega, Madison, WI, USA) for 10 min, rinsed with PBS for 5 min, and then immersed in blocking buffer (SuperBlock T20 solution; Thermo Scientific, Rockford, IL, USA) for 30 min. Sections were then incubated overnight at 4 °C in appropriate primary antibody: *fas* Ligand, c-kit/CD117 (Santa Cruz Biotech, Santa Cruz, CA, USA), cleaved caspase-8 and cleaved caspase-9

(Cell Signaling, Danvers, MA, USA). Secondary staining was performed with Alexa 488 or Alexa 546-conjugated IgG antibody (Invitrogen, San Diego, CA, USA) for 30 min. Controls included slides with no primary antibody and/or with isotype control. Cell nuclei were stained with DAPI. Imaging was performed using the Zeiss Laser scanning microscope 510-Meta confocal microscope.

Western Blots
We used our previously described immunoblotting protocol[6,7] to measure cleaved caspase-8 and cleaved caspase-9 in the intestine of sham/ECMO animals, and phospho-p38 mitogen-activated protein kinase (MAPK; thr180/tyr182) in mast cells (antibodies from Cell Signaling).

ELISA
Plasma intestinal fatty acid-binding protein (I-FABP) concentrations were measured using a commercially available ELISA kit (MyBioSource, San Diego, CA, USA) per manufacturer's protocol. The assay has a linear range of 78–5000 pg/ml.

Reverse Transcriptase-Quantitative PCR (RT-qPCR)
Messenger RNA expression of death receptor (DR) ligands was quantified using our previously described SYBR green protocol. Primers were designed using the Beacon Design software (Bio-Rad, Hercules, CA, USA; Table 1). Data were analyzed using the $2^{-\Delta\Delta CT}$ method.

Porcine Intestinal Mast Cells
Intestinal c-kit$^+$ FcεR1$^+$ mast cells were isolated by FACS sorting.[12] Briefly, intestinal tissue was rinsed with Hanks' balanced-salt solution (HBSS) containing 1 mM DTT (Sigma-Aldrich, St Louis, MO, USA) to remove adherent mucus, washed with HBSS containing 1 mM EDTA (Sigma) for 20 min twice at 37 °C, and then incubated in HBSS containing 1 mM collagenase type IV (Sigma) for 2 h at 37 °C. Cell suspensions were stained using FITC-conjugated monoclonal anti-human c-kit/CD117 (BD Biosciences, San Jose, CA, USA) and PE-conjugated anti-human FcεR1 antibodies (MyBiosource,

San Diego, CA, USA) and dual-positive cells were sorted by FACS. Phospho-p38 MAPK was measured in mast cells by FACS after permeabilizing (Cytofix/Cytoperm kit, BD Biosciences) and staining these cells with PE-conjugated mouse anti-p38 MAPK (thr180/tyr182; BD Biosciences). In some experiments, we treated mast cells with *Escherichia coli* LPS (0.1–1 μg/ml) and/or the p38 inhibitor SB202190 (Sigma) overnight and measured *fas* ligand expression by RT-qPCR.

Statistical Methods
Parametric and non-parametric tests were applied using the Sigma Stat 3.1.1 software (Systat, Point Richmond, CA, USA). For PCR data, crossing-threshold ($\Delta\Delta CT$) values were compared for genes with a ≥ 2-fold increase by Mann–Whitney U-test. Number of samples and statistical analyses is indicated in each figure legend. Each sample was tested in duplicate. A P value of < 0.05 was considered significant.

RESULTS
ECMO Is Associated with Intestinal Epithelial Cell Apoptosis
To investigate whether epithelial apoptosis has an early and underlying role in gut mucosal injury during ECMO, we first

Table 1 Primer sequences used for real-time reverse transcriptase-PCR

mRNA	Forward primer (5′→3′)	Reverse primer (3′→5′)
TNFSF1	TTCCAACAGTCTCATCTTCC	ATCCTCAGCAGAGCATCC
TNFSF2	TGCCTTGGTTCAGATGTG	GAGGTTCAGCGATGTAGC
TNFSF5	GACAAGGAATCTATTACATCTACG	AGAGGCTGGCTATGAAGG
TNFSF6	CCTGTGTCTCCTTGTGATG	GATGATTCTGTATGCCTTTGG
TNFSF7	ACATCCAGGTGACATTGAC	TGAAAGTTGAGGCGTAGC
TNFSF10	GACCCAGCAATCCCACTC	CACACCTTCTTAATCTATTCATCC
TNFSF12	GCCTCTCCCTCCGTGTAG	GAGTTGTCAGGACCGATGG

Figure 1 Extracorporeal membrane oxygenation (ECMO) is associated with apoptotic changes in intestinal epithelial cells. (**a**) Representative photomicrographs on the left show H&E-stained intestinal tissue (× 100) from sham- and ECMO-treated piglets after 2 h of treatment. Photomicrographs (× 1000) on the right show representative (A) sham villus; (B) sham crypt; (C) ECMO villus; and the (D) ECMO crypt. Many epithelial cells showed changes in nuclear morphology suggestive of apoptosis, such as clumping of chromatin, pyknosis, or nuclear fragmentation (black arrows), or peripheral condensation of chromatin (white arrows). (**b**) Tissues obtained after 8 h of ECMO (ordered similarly as in **a**) showed extensive epithelial exfoliation from villus tips (asterisk). In the crypts, many epithelial cells showed pyknosis (black arrows) or peripheral condensation of chromatin (white arrows). (**c**) Bar diagrams (means ± standard errors) show the percentage of epithelial nuclei with chromatin condensation in the sham and ECMO intestine after 2 h (top) and 8 h (bottom). In the 8 h intestine, no data are shown for villi because of extensive exfoliation of the villus epithelium. (**d**) H&E-stained intestinal tissue section (100 ×) from a full-term, 21-day-old human infant who died during ECMO shows similar loss of epithelium. (**e**) Representative fluorescence photomicrographs (× 630) show nuclear staining with 4′,6-diamidino-2-phenylindole (DAPI; blue) in the sham and ECMO intestine after 2 h and 8 h of treatment. Arrows indicate nuclei with chromatin fragmentation or peripheral condensation ('signet ring' appearance). The 8 h ECMO villus was denuded of epithelium (asterisk). High-magnification photomicrographs (× 2000, in the box on right) highlight nuclei that have undergone fragmentation (top) and peripheral chromatin condensation. Below, bar diagrams (means ± s.e.) depict (A) percentage of epithelial nuclei with chromatin condensation or fragmentation in the sham or ECMO intestine at 2 h and 8 h; (B) nuclear area in the sham *vs* ECMO intestine after 2 h of treatment; and (c) nuclear irregularity index in the sham *vs* ECMO intestine after 2 h. *$P < 0.05$, **$P < 0.01$, and ***$P < 0.001$.
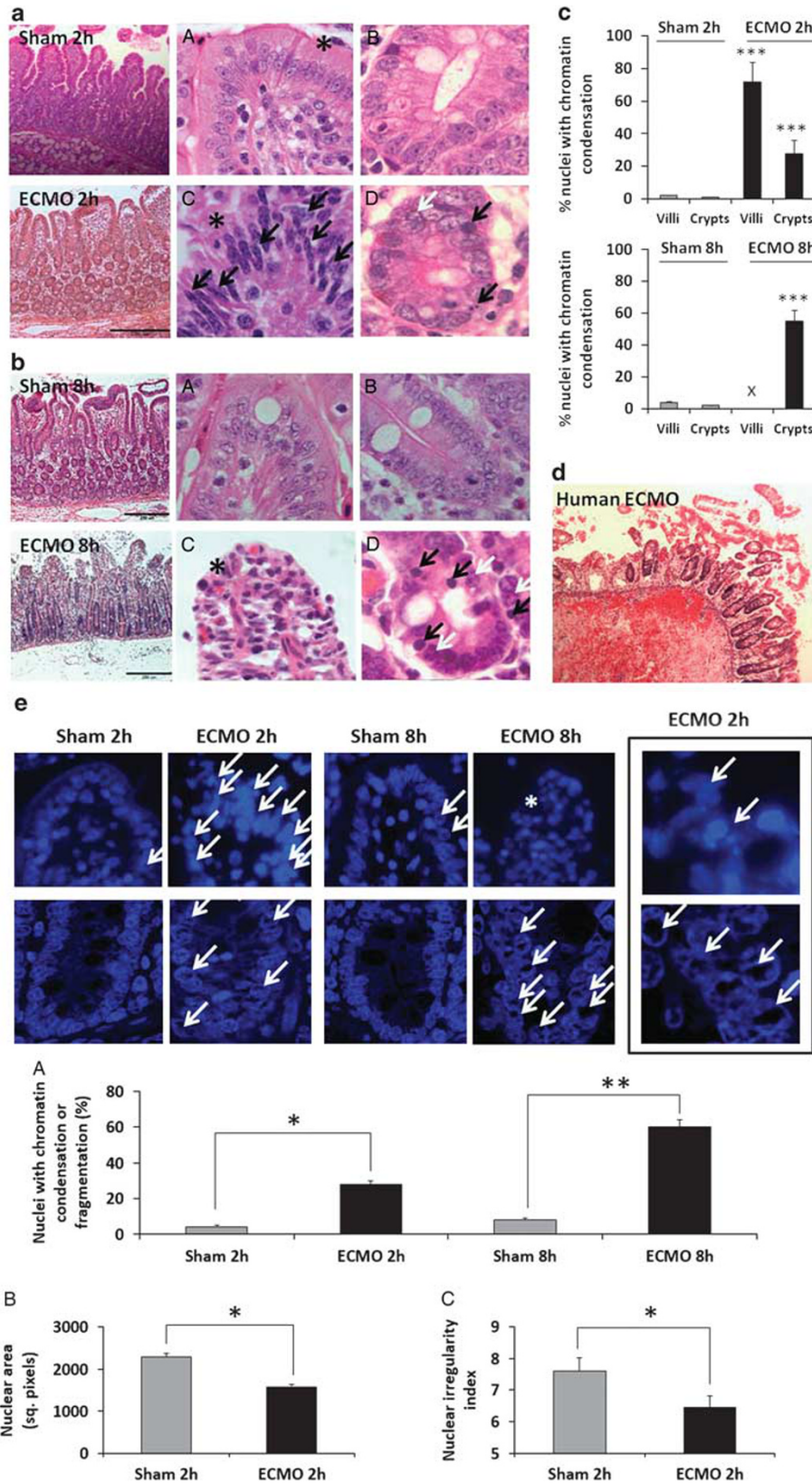
Figure 1 For caption refer page 152.

examined tissue sections of the small intestine (jejunum and ileum) from sham- and ECMO-treated piglets. As shown in Figure 1, nuclear morphological changes that are typically associated with apoptosis were notable in epithelial cells in ECMO- but not in the sham-treated intestine. After 2 h of ECMO, nuclei near the villus tips showed condensation of chromatin into distinct clumps. In the crypts, a few nuclei showed chromatin condensation, fragmentation, or pyknosis (Figure 1a and c). After 8 h of ECMO, most villi were completely denuded of epithelium. Most of the crypt epithelial cells showed apoptotic changes. These findings contrasted with the sham intestine, which did not show such apoptotic changes (Figure 1b and c). To determine whether these findings of gut epithelial injury in piglet ECMO were relevant to human infants receiving ECMO, we reviewed archived autopsy samples from neonates ($n = 10$) who died during ECMO. Tissue sections from all the 10 autopsies showed severe epithelial exfoliation in the gastrointestinal tract. A representative photomicrograph from a full-term infant who was treated with ECMO for intractable pulmonary hypertension and died during treatment is depicted in Figure 1d.

To confirm whether ECMO was associated with apoptosis in intestinal epithelial cells, we examined the nuclear morphology in DAPI-stained sections and also performed TUNEL staining. As shown in Figure 1e, apoptotic changes were detectable after 2 h of ECMO. Nuclear fragmentation was a frequent finding in epithelial cells near the villus tips, whereas crypt cells showed peripheral condensation of chromatin (Figure 1eA). These findings indicated that the apoptotic changes were at a more advanced stage near villus tips than in the crypts. After 8 h of ECMO, a majority of crypt epithelial cells showed chromatin condensation. We also compared the nuclear geometry in epithelial cells in sham and ECMO intestine using computational image analysis. ECMO was associated with a reduction in nuclear area (2286.36 ± 238.4 in sham *vs* 1586.39 ± 106.89 square pixels in the ECMO intestine, $P < 0.05$; Figure 1eB). We computed a NII, which includes nuclear area, the ratio of its major and minor radii, ratio of its area to the area of its bounding box, ratio of its major and minimum radii, and nuclear roundness. ECMO was associated with lower NII values (7.59 ± 0.4 in sham intestine *vs* 6.45 ± 0.3 in ECMO, $P < 0.05$; Figure 1eC). These findings were suggestive of early apoptosis, which is typically associated with nuclear condensation and increased regularity of the nuclear outline.

TUNEL staining further supported our findings of apoptotic changes in the epithelium. As shown in Figure 2a, TUNEL$^+$ nuclei were seen all along the villus tip and in some crypt cells at the 2 h time point. Finally, to confirm that epithelial apoptosis preceded villous damage during ECMO, we scored serial tissue sections for the severity of epithelial apoptosis and the severity of villous damage. Changes limited to villus tips received a score of 1, whereas involvement of the entire crypt-villus axis was scored as 4. As depicted in
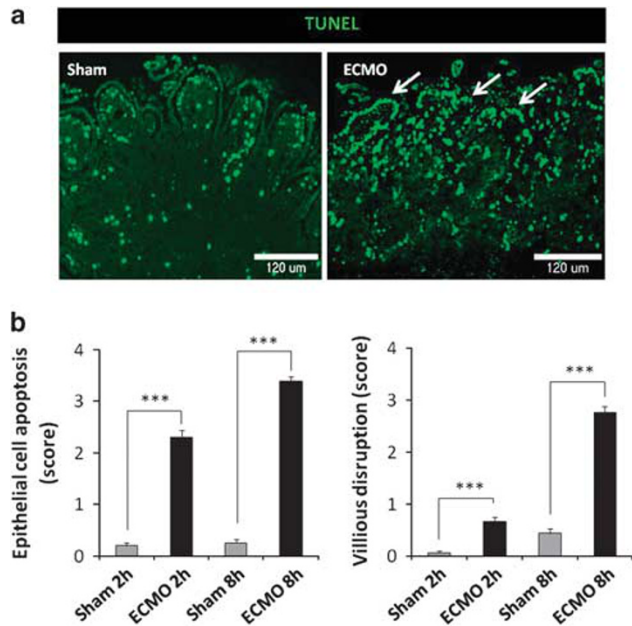

Figure 2 Epithelial cell apoptosis precedes villus injury during extracorporeal membrane oxygenation (ECMO). (**a**) Representative photomicrographs show TUNEL staining (green) that confirmed increased intestinal epithelial cell apoptosis in the ECMO intestine compared with sham after 2 h of treatment (arrows); (**b**) Bar diagrams (means ± standard error) show epithelial cell apoptosis (score) and the villus disruption (score) in serial sections from the sham- and ECMO-treated intestine. Data represent $n = 5$ animals per group. ***$P < 0.001$.

Figure 2b, apoptosis scores increased before the onset of villous damage after 2 h of ECMO.

Plasma I-FABP Concentrations Are Increased during ECMO

Because swelling of villus tips and exfoliation of epithelial cells from villi can be a part of the postmortem/autolytic changes in the intestine,[13,14] we sought additional evidence that epithelial injury we noted in the ECMO intestine occurred while the animal was alive and during ECMO. Tissue sections were carefully screened and confirmed to be negative for other signs of autolysis such as hemolysis of red blood cells and the loss of differential staining in various layers. To investigate whether epithelial cell death occurred during ECMO, we measured serial plasma concentrations of I-FABP, a cytosolic protein uniquely located in mature enterocytes and a sensitive biochemical marker of early gut mucosal injury. As depicted in Figure 3, I-FABP levels started rising soon after the initiation of ECMO and increased progressively during the 8 h ECMO run.

ECMO Activates the Extrinsic Pathway of Apoptosis in Intestinal Epithelial Cells

We next investigated the mechanism by which gut epithelial cells undergo apoptosis during ECMO. To determine the
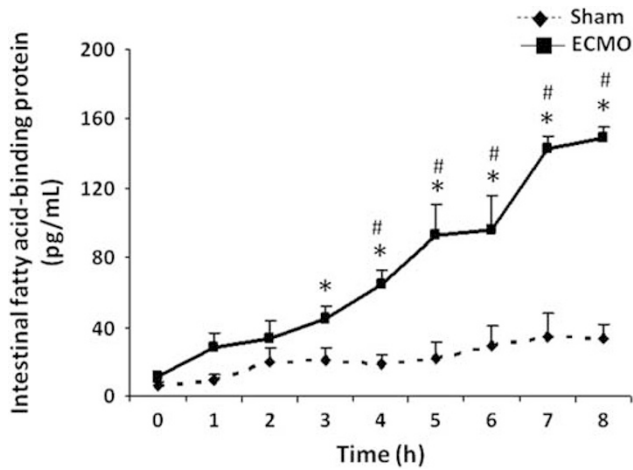
Figure 3 Circulating intestinal fatty acid-binding protein concentrations are increased during extracorporeal membrane oxygenation (ECMO). Line diagram (means ± standard error) shows plasma concentrations of intestinal fatty acid-binding protein in sham- and ECMO-treated piglets. Data represent $n = 8$ animals per group. $* < 0.05$ compared with sham (Kruskal–Wallis H-test); $^{#}P < 0.05$ compared with baseline measurement in ECMO animals (repeated measures analysis by Friedman test).

signaling pathway(s) involved in this process, we immunostained the sham and ECMO intestine for cleaved caspase-8, which is typically associated with the extrinsic, DR-linked pathway, and cleaved caspase-9, which is involved in the mitochondrial-related intrinsic pathway. We detected prominent epithelial immunoreactivity for cleaved caspase-8, but not cleaved caspase-9, in the ECMO intestine. The sham intestine did not stain for either of the two markers (Figure 4a). To confirm these findings, we performed western blots on tissue samples from sham and ECMO intestine. Unlike sham, ECMO intestine showed increased expression of the intermediate form of caspase-8, p43/p41, and of the active, cleaved fragment, p18 (Figure 4b). There was no change in the full-length caspase-9 protein or its active p35 fragment.

ECMO Induces Fas Ligand Expression in the Intestinal Mast Cells

To investigate the mechanisms underlying the activation of caspase-8 in the intestinal epithelium during ECMO, we first used RT-qPCR to measure the gene expression of DR ligands that are known to be associated with gut mucosal injury and have been characterized in swine. As depicted in Figure 5a, ECMO was associated with increased expression of *fas* ligand/TNF superfamily, member 6 (TNFSF6), TNF-related apoptosis-inducing ligand (TRAIL)/TNFSF10, and TNF/TNFSF2. We have previously described increased expression of TNF during ECMO. There was also a trend toward increased CD40 ligand/TNFSF5 that did not reach significance. In the present study, we focused on *fas* ligand in subsequent experiments.
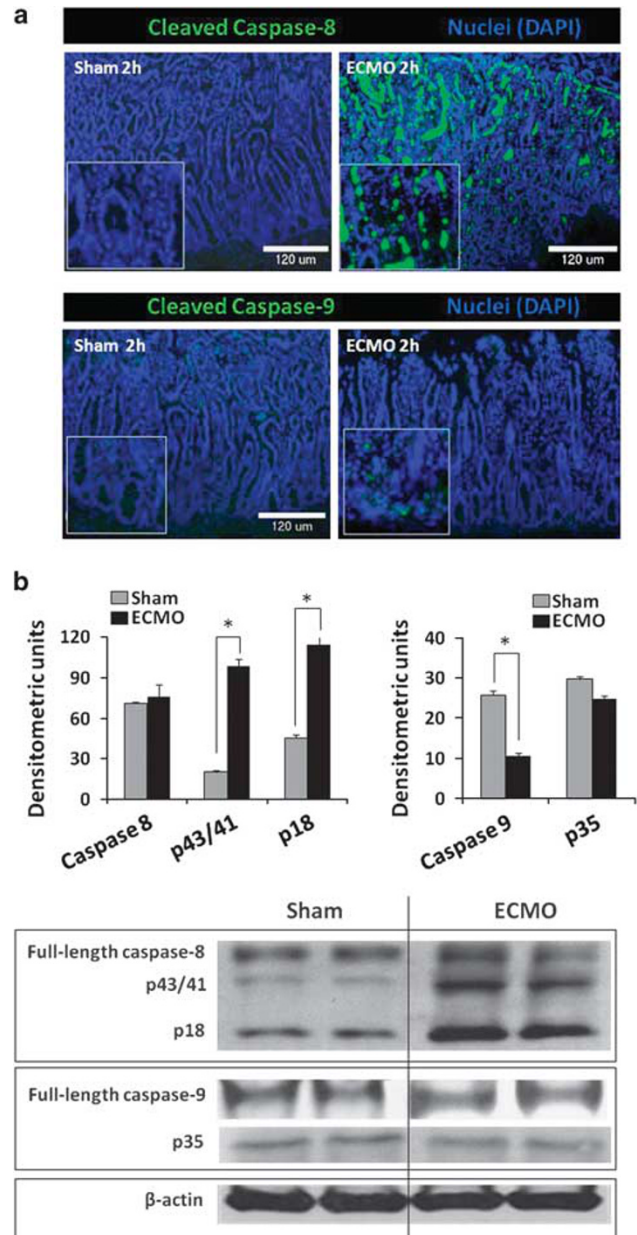

Figure 4 Extracorporeal membrane oxygenation (ECMO) activates the extrinsic pathway of apoptosis in intestinal epithelial cells. (**a**) Representative fluorescence photomicrographs from sham- and ECMO-treated piglet intestine after 2 h of treatment show immunoreactivity for cleaved caspase-8 (A), but not for cleaved caspase-9 (B), in intestinal epithelial cells. Nuclear staining (blue) was obtained with 4′,6-diamidino-2-phenylindole (DAPI). (**b**) Representative western blots show cleaved caspase-8 and cleaved caspase-9 expression in the sham and ECMO intestine after treatment for 2 h. *Upper box:* ECMO intestine showed increased expression of the intermediate form of caspase-8, p43/p41, and of the active, cleaved fragment, p18. *Middle box:* ECMO was associated with caspase-9, with no change in cleaved caspase-9 (p35). *Lower box:* β-actin expression (housekeeping gene). Bar diagrams (means ± s.e.) show summarized densitometric data. Data represent $n = 5$ animals per group. $*P < 0.05$.
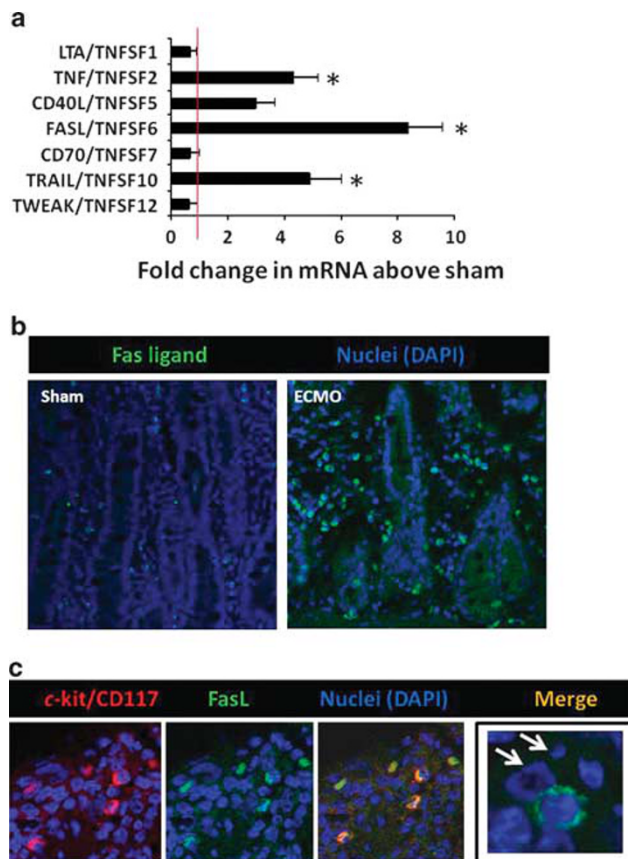
Figure 5 Extracorporeal membrane oxygenation (ECMO) induces *fas* ligand expression in the intestinal mast cells. (**a**) Bar diagram (means ± s.e.) shows fold change in mRNA expression of major death receptor ligands in sham- and ECMO-treated porcine intestine after treatment for 2 h. ECMO was associated with a significant increase in *fas* ligand, TRAIL, and TNF expression. (**b**) Fluorescence photomicrographs (× 100) show increased immunoreactivity for *fas* ligand (green) in the ECMO intestine. Nuclear staining (blue) was obtained with 4′,6-diamidino-2-phenylindole (DAPI). (**c**) Fluorescence photomicrographs (× 400) localize *fas* ligand (green) in *c*-kit/CD117 + mast cells (red) present in the *lamina propria*. Inset shows a *fas* ligand-expressing mast cell in close proximity to an apoptotic epithelial cell (arrows). Data are representative of n = 5 animals in sham and ECMO groups. *P < 0.05.

To identify the cellular source(s) of *fas* ligand in the intestine during ECMO, we next performed immunohistochemistry on tissue sections from the sham and ECMO intestine. As shown in Figure 5b, ECMO was associated with increased immunoreactivity for *fas* ligand in *lamina propria* mast cells, which were identifiable by their prominent cytoplasmic granules and positive staining for *c*-kit/CD117. Consistent with the hypothesis that *fas* ligand promotes epithelial apoptosis during ECMO, many *c*-kit/CD117 + *fas* ligand + mast cells could be identified in close proximity to epithelial nuclei that showed morphological changes of apoptosis (Figure 5c).

P38 MAPK Drives Fas Ligand Expression in Mast Cells in the ECMO Intestine

To determine the mechanisms driving *fas* ligand expression in intestinal mast cells, we focused on the role of p38 mitogen-activated protein kinase. Existing data implicate p38 activation in a wide range of mast cell functions, including differentiation, inflammatory activation, and degranulation.[15,16] We first measured phospho-p38 expression in mast cells isolated from the sham and ECMO intestine by flow cytometry (Figure 6a). This antibody detects p38 that is dual phosphorylated at the thr180 and tyr182 residues. Consistent with these findings, phospho-p38 was immunolocalized in c-kit/CD117 + mast cells in ECMO, but not in the sham intestine (Figure 6b).

We have previously demonstrated that ECMO is associated with epithelial barrier dysfunction and bacterial translocation.[7] Based on these observations, we hypothesized that increased exposure to bacterial products can induce p38-mediated *fas* ligand expression in intestinal mast cells during ECMO. To investigate this possibility, we treated mast cells from the normal piglet intestine with *E. coli* LPS *in vitro*, and as shown in western blots in Figure 6c, LPS promoted p38 phosphorylation in these cells. LPS also increased *fas* ligand expression in mast cells, which was blocked by prior exposure to SB202190, a specific small-molecule inhibitor of p38 MAPK (Figure 6d). These data emphasize the role of p38-mediated signaling in the induction of *fas* ligand in mast cells.

DISCUSSION

We present a detailed investigation into the timing and mechanisms of gut epithelial injury during ECMO. In our piglet model of ECMO, epithelial apoptosis preceded villous damage and continued throughout the 8 h course of the study. We show that the extrinsic apoptotic pathway is at play in the epithelium, with evidence of increased expression of *fas* ligand and related DR ligands by *lamina propria* mast cells. Finally, we show that the ECMO was associated with activation of p38 MAPK in intestinal mast cells, which induced *fas* ligand expression in these cells. To our knowledge, this is the first study to investigate the mechanisms of gut epithelial injury in extracorporeal circulation.

In our piglet model, we detected extensive epithelial apoptosis after 2 h of ECMO. We chose a cautious approach and sought multiple lines of evidence to confirm apoptotic changes because of concerns that in necrotic tissue injury, a single test such as TUNEL may not be adequate for accurate estimation of apoptosis.[17–20] Although the effects of extracorporeal circulation on the gut epithelium are not well documented, increased epithelial apoptosis has been described in diverse gastrointestinal conditions such as ischemia-reperfusion (I/R) injury, necrotizing enterocolitis, infectious diarrhea, celiac disease, and inflammatory bowel disease.[11,21–24] Interestingly, epithelial apoptosis in our model of piglet ECMO followed a pattern similar to intestinal I/R injury,
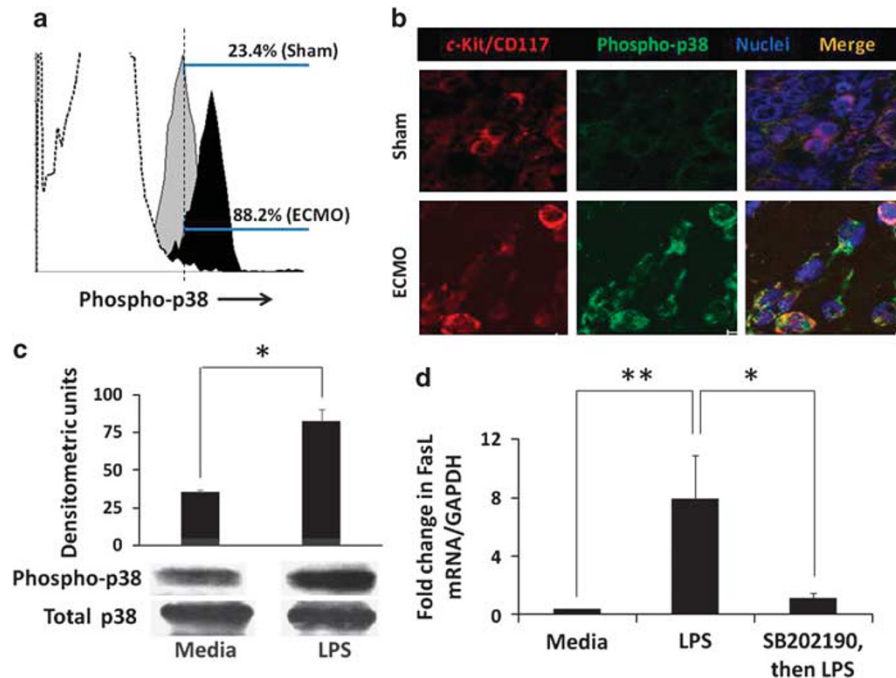
Figure 6 Activation of p38 MAPK has a key role in *fas* ligand production in mast cells in the extracorporeal membrane oxygenation (ECMO) intestine. (**a**) ECMO is associated with increased phospho-p38 expression in intestinal mast cells. Representative histograms obtained by FACS analysis show phospho-p38 expression in intestinal mast cells from sham and ECMO piglets, obtained after 2 h of treatment. (**b**) Fluorescent photomicrographs (× 630) show that phospho-p38 (green) was immunolocalized in c-kit/CD117$^+$ mast cells (red). Data represent $n = 5$ animals in sham and ECMO groups. (**c**) Representative western blots show that LPS-treatment of mast cells isolated from normal piglet intestine *ex vivo* promotes p38 phosphorylation in these cells. Bar diagram (means ± s.e.) shows summarized densitometric data. (**d**) Bar diagram (means ± s.e.) shows fold change in fas ligand mRNA expression in intestinal mast cells (isolated from normal piglet intestine) in the native state, after treatment with LPS (1 μg/ml), and with SB202190 (1 μM) before LPS treatment. Data represent three separate experiments. *$P < 0.05$, **$P < 0.01$.

where apoptotic changes occur earlier and are more extensive at villus tips than in the crypts. Similar to the clinical experience during human ECMO, piglets receiving ECMO frequently developed tachycardia and hypotension within 1–2 h of initiation of the procedure, which responded to intravenous fluid boluses.[6] In these animals, even though hemodynamic parameters were maintained in the normal range with aggressive fluid resuscitation, subclinical gut ischemia due to the redistribution of blood flow to vital organs is plausible. Besides direct effects of extracorporeal circulation, I/R is also a plausible contributor to bowel injury during both ECMO and CPB because both modalities are often used in infants with cardiopulmonary failure who may have had varying degrees of intestinal hypoperfusion before the initiation of the procedure. During venoarterial ECMO, significant hemodynamic changes have been documented because of the loss of pulsatile blood flow and during times when the bridge between the venous drainage and the infusion tubing is opened.[25] During CPB, intra-operative cardioplegia, aortic cross-clamping, hypothermia, and hemo-dilution can add to the risk of intestinal I/R.[26–29] Although the pathophysiological significance of epithelial apoptosis in the ECMO-related bowel injury remains uncertain, it is known to have a central role in intestinal I/R injury; in

preclinical models, strategies to prevent gut epithelial apoptosis such as pre-treatment with caspase inhibitors or gut epithelial-specific overexpression of bcl-2 have been shown to reduce the severity of histopathological damage.[30]

ECMO was associated with increased expression of cleaved caspase-8 in intestinal epithelium, indicating that the extrinsic pathway of apoptosis was activated in these cells. Caspase-8 is a cysteine protease that initiates apoptosis in response to cell surface receptors of the TNF receptor superfamily called the DRs.[31] To trigger cell death, DRs recruit an adaptor protein, the *fas*-associated protein with a death domain, which then activates the caspase-8 pro-enzyme, leading to the activation of downstream caspases 3, 6, and 7, and apoptosis.[32] In a previous report, we had shown that ECMO was associated with activation of intestinal mast cells, which released pre-formed TNF.[6] However, when all the DR ligands were measured simultaneously in the present study, *fas* ligand was the most highly expressed gene in this superfamily. Besides direct activation of DR-mediated signaling, DR ligands can also activate the extrinsic apoptotic pathway indirectly in epithelial cells through cytoskeletal condensation and disruption of the tight junctions. Dissolution of tight junctions can release occludin, which can serve as a non-canonical DR ligand to activate the extrinsic pathway.[33]
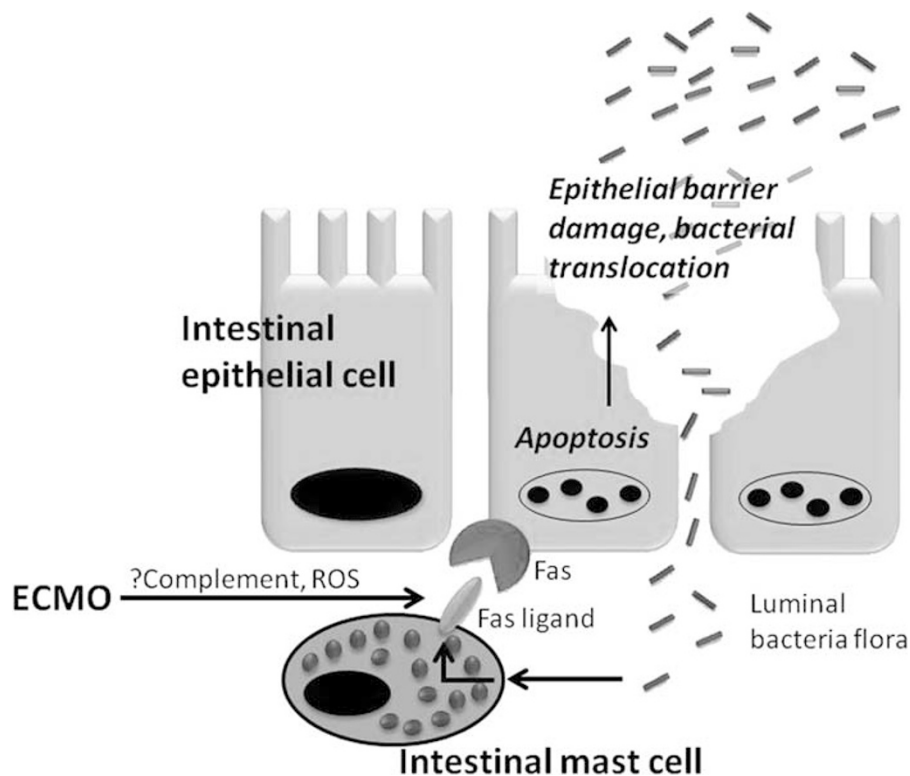
Figure 7 Schematic showing the proposed pathophysiological model for intestinal epithelial cell apoptosis during extracorporeal membrane oxygenation (ECMO). ECMO-induced mast cell degranulation releases *fas* ligand, which triggers intestinal epithelial cell apoptosis, epithelial barrier disruption, and bacterial translocation. These bacterial products then activate p38 MAPK to promote sustained expression of *fas* ligand in mast cells, thereby setting up a feed-forward cycle of epithelial damage, bacterial translocation, and mast cell activation.

Fas ligand has been implicated in gut epithelial apoptosis in several diseases, including I/R, Crohn's disease, ulcerative colitis, celiac disease, and graft *vs* host disease.[34,35] *Fas* ligand ligates its cognate receptor, *fas*/CD95, which is constitutively expressed on the basolateral surface of epithelial cells.[23,36,37] Following ligation of *fas*, caspase-8 activation results in the formation of a hetero-tetramer comprised of two units each of the enzymatically active caspase-8 fragments, p18 and p10.[31] Two pathways have been described:[38] the type I pathway is invoked by membrane-bound *fas* ligand and results in the formation of relatively copious amounts of the caspase-8 hetero-tetramers. The type II pathway overlaps with the intrinsic apoptotic pathway and is often seen in T lymphoblasts such as Jurkat cells, where membrane-bound or soluble *fas* ligand activates the pro-apoptotic protein *bid* (BH3 interacting-domain death agonist), which results in mitochondrial damage and apoptosis.[39] Intestinal epithelial cells generally display type I-like characteristics with activation with formation of large amounts of the active caspase-8 fragments.[40] However, an important caveat for the role of *fas* ligand is that despite its identification as the trigger for epithelial apoptosis in various diseases, its pathophysiological significance in gut mucosal injury remains unproven because mice with deficiencies in *fas* and

fas ligand do not seem to be protected in chemical colitis models.[41]

We have identified mast cells as the primary cellular source of *fas* ligand in the ECMO intestine. These findings are consistent with our previous observations that ECMO is associated with degranulation and activation of intestinal mast cells, which rapidly release inflammatory mediators such as TNF, tryptase, and chymase locally and into the circulation.[6,7] Mast cells also release inflammatory mediators, including *fas* ligand, in exosomes.[42] Intestinal mast cells are increasingly recognized as a major source of pre-formed inflammatory mediators in SIRS in diverse settings such as in Gram-negative and Gram-positive bacterial sepsis, peritonitis, severe alveolar hypoxia, and portal hypertension.[43–47] Although the initial trigger for intestinal epithelial cell apoptosis in our model remains unclear, we speculate that pre-formed stores of *fas* ligand in mast cells may have a role. Once the epithelial barrier is disrupted, increased exposure to bacterial products can explain p38-mediated *fas* ligand expression in mast cells, and a feed-forward cycle of epithelial damage, bacterial translocation, and mast cell activation (Figure 7).

Elucidation of the inflammatory pathways involved in extracorporeal circulation-related SIRS is a critical step in the

development of effective anti-inflammatory therapies. Extracorporeal circulation-related SIRS cannot be prevented merely by improvements in the membrane oxygenator or the circuit. Physical characteristics of the ECMO/CPB circuit such as fluid dynamics, blood volume-to-surface area ratio, and the material's affinity for fibrinogen determine its propensity for contact activation of inflammatory pathways.[48] Although smoother circuits can be designed, the structure of the membrane oxygenator calls for conflicting profiles—the necessity for the gas exchange obligates thin blood films and turbulence, factors that also favor contact activation. Thus, even though improved silicone oxygenators have shown modest benefit in reducing platelet and contact activation, these improvements face a mathematical bottleneck where reduction in turbulence and blood surface interaction compete with the gas exchange capacity of the oxygenator.[49] We have identified caspase-8-mediated epithelial apoptosis and intestinal mast cells as potentially important pathophysiological mediators in ECMO-related bowel injury, which can accentuate the SIRS through increased systemic exposure to bacterial products. Further study is needed in patients receiving ECMO/CPB to determine the kinetics and significance of these events during human ECMO.

DISCLOSURE/CONFLICT OF INTEREST
The authors declare no conflicts of interest.

1. Chen Q, Yu W, Shi J, et al. The effect of venovenous extra-corporeal membrane oxygenation (ECMO) therapy on immune inflammatory response of cerebral tissues in porcine model. J Cardiothorac Surg 2013;8:186.
2. Halter J, Steinberg J, Fink G, et al. Evidence of systemic cytokine release in patients undergoing cardiopulmonary bypass. J Extra Corpor Technol 2005;37:272–277.
3. Mildner RJ, Taub N, Vyas JR, et al. Cytokine imbalance in infants receiving extracorporeal membrane oxygenation for respiratory failure. Biol Neonate 2005;88:321–327.
4. Ichiba S, Bartlett RH. Current status of extracorporeal membrane oxygenation for severe respiratory failure. Artif Organs 1996;20:120–123.
5. Paden ML, Conrad SA, Rycus PT, et al. Extracorporeal Life Support Organization Registry Report 2012. ASAIO J 2013;59:202–210.
6. Mc IRB, Timpa JG, Kurundkar AR, et al. Plasma concentrations of inflammatory cytokines rise rapidly during ECMO-related SIRS due to the release of preformed stores in the intestine. Lab Invest 2010;90:128–139.
7. Kurundkar AR, Killingsworth CR, McIlwain RB, et al. Extracorporeal membrane oxygenation causes loss of intestinal epithelial barrier in the newborn piglet. Pediatr Res 2010;68:128–133.
8. Kerr JF, Wyllie AH, Currie AR. Apoptosis: a basic biological phenomenon with wide-ranging implications in tissue kinetics. Br J Cancer 1972;26:239–257.
9. Filippi-Chiela EC, Oliveira MM, Jurkovski B, et al. Nuclear morphometric analysis (NMA): screening of senescence, apoptosis and nuclear irregularities. PLoS One 2012;7:e42522.
10. Schneider CA, Rasband WS, Eliceiri KW. NIH Image to ImageJ: 25 years of image analysis. Nat Methods 2012;9:671–675.
11. Jilling T, Lu J, Jackson M, et al. Intestinal epithelial apoptosis initiates gross bowel necrosis in an experimental rat model of neonatal necrotizing enterocolitis. Pediatr Res 2004;55:622–629.
12. Sellge G, Bischoff SC. Isolation, culture, and characterization of intestinal mast cells. Methods Mol Biol 2006;315:123–138.
13. Pearson GR, Logan EF. Scanning electron microscopy of early postmortem artefacts in the small intestine of a neonatal calf. Br J Exp Pathol 1978;59:499–503.
14. Thorpe E, Thomlinson JR. Autolysis and post-mortem bacteriological changes in the alimentary tract of the pig. J Pathol Bacteriol 1967;93:601–610.
15. Zhang C, Baumgartner RA, Yamada K, et al. Mitogen-activated protein (MAP) kinase regulates production of tumor necrosis factor-alpha and release of arachidonic acid in mast cells. Indications of communication between p38 and p42 MAP kinases. J Biol Chem 1997;272:13397–13402.
16. Feoktistov I, Goldstein AE, Biaggioni I. Role of p38 mitogen-activated protein kinase and extracellular signal-regulated protein kinase kinase in adenosine A2B receptor-mediated interleukin-8 production in human mast cells. Mol Pharmacol 1999;55:726–734.
17. Kelly KJ, Sandoval RM, Dunn KW, et al. A novel method to determine specificity and sensitivity of the TUNEL reaction in the quantitation of apoptosis. Am J Physiol Cell Physiol 2003;284:C1309–C1318.
18. Tamura T, Said S, Lu W, et al. Specificity of TUNEL method depends on duration of fixation. Biotech Histochem 2000;75:197–200.
19. Zhao J, Schmid-Kotsas A, Gross HJ, et al. Sensitivity and specificity of different staining methods to monitor apoptosis induced by oxidative stress in adherent cells. Chin Med J (Engl) 2003;116:1923–1929.
20. Yasuhara S, Zhu Y, Matsui T, et al. Comparison of comet assay, electron microscopy, and flow cytometry for detection of apoptosis. J Histochem Cytochem 2003;51:873–885.
21. Ramachandran A, Madesh M, Balasubramanian KA. Apoptosis in the intestinal epithelium: its relevance in normal and pathophysiological conditions. J Gastroenterol Hepatol 2000;15:109–120.
22. Iwamoto M, Koji T, Makiyama K, et al. Apoptosis of crypt epithelial cells in ulcerative colitis. J Pathol 1996;180:152–159.
23. Ciccocioppo R, Di Sabatino A, Parroni R, et al. Increased enterocyte apoptosis and Fas-Fas ligand system in celiac disease. Am J Clin Pathol 2001;115:494–503.
24. Chen LW, Egan L, Li ZW, et al. The two faces of IKK and NF-kappaB inhibition: prevention of systemic inflammation but increased local injury following intestinal ischemia-reperfusion. Nat Med 2003;9:575–581.
25. Van Heijst A, Liem D, Van Der Staak F, et al. Hemodynamic changes during opening of the bridge in venoarterial extracorporeal membrane oxygenation. Pediatr Crit Care Med 2001;2:265–270.
26. Peek GJ, Firmin RK. The inflammatory and coagulative response to prolonged extracorporeal membrane oxygenation. ASAIO J 1999;45:250–263.
27. Caputo M, Bays S, Rogers CA, et al. Randomized comparison between normothermic and hypothermic cardiopulmonary bypass in pediatric open-heart surgery. Ann Thorac Surg 2005;80:982–988.
28. Asimakopoulos G. Systemic inflammation and cardiac surgery: an update. Perfusion 2001;16:353–360.
29. Brix-Christensen V. The systemic inflammatory response after cardiac surgery with cardiopulmonary bypass in children. Acta Anaesthesiol Scand 2001;45:671–679.
30. Coopersmith CM, O'Donnell D, Gordon JI. Bcl-2 inhibits ischemia-reperfusion-induced apoptosis in the intestinal epithelium of transgenic mice. Am J Physiol 1999;276:G677–G686.
31. Hoffmann JC, Pappa A, Krammer PH, et al. A new C-terminal cleavage product of procaspase-8, p30, defines an alternative pathway of procaspase-8 activation. Mol Cell Biol 2009;29:4431–4440.
32. Cabal-Hierro L, Lazo PS. Signal transduction by tumor necrosis factor receptors. Cell Signal 2012;24:1297–1305.
33. Beeman NE, Baumgartner HK, Webb PG, et al. Disruption of occludin function in polarized epithelial cells activates the extrinsic pathway of apoptosis leading to cell extrusion without loss of transepithelial resistance. BMC Cell Biol 2009;10:85.
34. An S, Hishikawa Y, Koji T. Induction of cell death in rat small intestine by ischemia reperfusion: differential roles of Fas/Fas ligand and Bcl-2/Bax systems depending upon cell types. Histochem Cell Biol 2005;123:249–261.
35. Inagaki-Ohara K, Nishimura H, Sakai T, et al. Potential for involvement of Fas antigen/Fas ligand interaction in apoptosis of epithelial cells by

intraepithelial lymphocytes in murine small intestine. Lab Invest 1997;77:421–429.

36. Abreu MT, Palladino AA, Arnold ET, *et al.* Modulation of barrier function during Fas-mediated apoptosis in human intestinal epithelial cells. Gastroenterology 2000;119:1524–1536.

37. Ueyama H, Kiyohara T, Sawada N, *et al.* High Fas ligand expression on lymphocytes in lesions of ulcerative colitis. Gut 1998;43:48–55.

38. Jost PJ, Grabow S, Gray D, *et al.* XIAP discriminates between type I and type II FAS-induced apoptosis. Nature 2009;460:1035–1039.

39. Kantari C, Walczak H. Caspase-8 and bid: caught in the act between death receptors and mitochondria. Biochim Biophys Acta 2011;1813: 558–563.

40. Pinkoski MJ, Brunner T, Green DR, *et al.* Fas and Fas ligand in gut and liver. Am J Physiol Gastrointest Liver Physiol 2000;278:G354–G366.

41. Park SM, Chen L, Zhang M, *et al.* CD95 is cytoprotective for intestinal epithelial cells in colitis. Inflamm Bowel Dis 2010;16:1063–1070.

42. Zuccato E, Blott EJ, Holt O, *et al.* Sorting of Fas ligand to secretory lysosomes is regulated by mono-ubiquitylation and phosphorylation. J Cell Sci 2007;120:191–199.

43. Mallen-St Clair J, Pham CT, Villalta SA, *et al.* Mast cell dipeptidyl peptidase I mediates survival from sepsis. J Clin Invest 2004;113: 628–634.

44. Sutherland RE, Olsen JS, McKinstry A, *et al.* Mast cell IL-6 improves survival from Klebsiella pneumonia and sepsis by enhancing neutrophil killing. J Immunol 2008;181:5598–5605.

45. Nautiyal KM, McKellar H, Silverman AJ, *et al.* Mast cells are necessary for the hypothermic response to LPS-induced sepsis. Am J Physiol Regul Integr Comp Physiol 2009;296:R595–R602.

46. Chao J, Wood JG, Gonzalez NC. Alveolar hypoxia, alveolar macrophages, and systemic inflammation. Respir Res 2009;10:54.

47. Tang CW, Lan C, Liu R. Increased activity of the intestinal mucosal mast cells in rats with multiple organ failure. Chin J Dig Dis 2004;5: 81–86.

48. Hennessy Jr VL, Hicks RE, Niewiarowski S, *et al.* Function of human platelets during extracorporeal circulation. Am J Physiol 1977;232: H622–H628.

49. Baier RE. The organization of blood components near interfaces. Ann N Y Acad Sci 1977;283:17–36.